International Journal of Technology 15(6) 1971-1981 (2024)
Received January 2023 / Revised January 2023 / Accepted February 2023

International Journal of Technology

http://ijtech.eng.ui.ac.id

Improvement of an Anode-Supported Intermediate Temperature Solid Oxide Fuel Cell with Spray-Coated Calcia-Stabilized Zirconia Electrolytes

Fauzi Yusupandi[1,2], Muhammad Ilham[1], Ilham Ali Yafi[1], Pramujo Widiatmoko[1], Isdiriayani Nurdin[1], Saumi Febrianti Khairunnisa[1], Hary Devianto[1*]

[1]*Department of Chemical Engineering, Faculty of Industrial Technology, Institut Teknologi Bandung, Jl. Ganesha No. 10, Bandung 40132, Indonesia*
[2]*Department of Chemical Engineering, Institut Teknologi Sumatera, Jl. Terusan Ryacudu, Way Huwi, Kec. Jati Agung, Lampung Selatan 35365, Indonesia*

Abstract. Among the three types of Solid Oxide Fuel Cell (SOFC), intermediate temperature solid oxide fuel cells (IT-SOFC) have been widely developed due to reducing operating costs and materials. In this study, we produced an anode-supported IT-SOFC cell through the dry-pressing method for NiO-CSZ anode production and spray coating technique for Calcia-Stabilized Zirconia (CSZ) electrolyte and calcium cobalt zinc oxide (CCZO)-CSZ cathode fabrication. A single cell was enhanced by changing the anode's composition, increasing the sintering temperature, using a ball mill as mixing equipment, and multiplying the coating of the electrolyte. The cell with eight times of electrolyte coating had a greater peak power density than that of one time of electrolyte coating even though the curvature of eight times of electrolyte coating was higher. Additionally, the cell performance with eight times of electrolyte achieved the peak power density of 0.24; 0.35; and 1.08 mW/cm^2 and the ohmic resistance of 168.3; 90.10; and 26.78 Ω at the operating temperature of 600, 700, and 800 °C, respectively.

Keywords: Anode-supported; Calcia Stabilized Zirconia (CSZ); Curvature; IT-SOFC; Spray coating

1. Introduction

Fuel cell directly transforms the chemical energy of various fuels and an oxidant (often air) into electricity and heat without burning the fuel. The advantages of fuel cells are high electrical efficiency, silent operation, and little or no emission (Sazali *et al.,* 2020; Wang and Jiang, 2017). Solid oxide fuel cell (SOFC) is one of the highly promising fuel cells in small to large-scale power plant applications. SOFC is classified as a high-temperature fuel cell operated between 800 and 1,000 °C. Unlike low-temperature fuel cells (PEMFCs), which need pure hydrogen as fuel, fossil or renewable fuels such as natural gas and bioethanol can be used directly in SOFC through internal reforming. Moreover, noble metals are unnecessary for SOFC's electrode materials since the high operating temperature enhances the reaction kinetics of electrodes (Shi *et al.,* 2020; Kaur and Singh, 2020). However, the production and operation cost of conventional SOFC is too high due to complex materials and high heat requirements. To overcome these drawbacks, the operating temperature of

*Corresponding author's email: hardev@itb.ac.id, Tel.: +6222504551, Fax.: +62222509406
doi: 10.14716/ijtech.v15i6.6308

the recent SOFC decreases to 500 – 800 °C, called an intermediate-temperature SOFC (IT-SOFC) (Baharuddin, Muchtara, and Somalu, 2017).

The main parts of the SOFC cell are a porous cermet anode, a dense ceramic electrolyte, and a porous oxide-based cathode. NiO is frequently used as an anode material which has great electrical conductivity and oxidation kinetics of hydrogen (Abdalla *et al.,* 2018; Singhal and Kendall, 2003). On the other hand, the common cathode material is lanthanum-based oxide composites such as lanthanum strontium manganite (LSM) and lanthanum cobalt ferrite (LSCF). However, the side reaction of lanthanum-based cathode and zirconia-based electrolyte can occur at high temperatures to form a high-resistance product (Chen *et al.,* 2014). Nowadays, calcium- and cobalt-based materials such as calcium cobalt oxide (CCO) and calcium cobalt zinc oxide (CCZO) is prospective cathodes in IT-SOFC owing to low cost, great oxygen reduction activity, suitable thermal expansion with electrolyte materials and thermoelectric behavior to utilize waste heat to electricity (Yu *et al.,* 2017; Takami and Ikuta, 2005). Additionally, yttria-stabilized zirconia (YSZ) is widely used as an electrolyte in SOFC systems (Rahmawati *et al.,* 2017). However, yttria is costly and has low reserves associated with rare earth materials. Calcia (CaO) can be an alternative stabilizer to maintain the cubic phase of zirconia at all temperatures (Kurapova *et al.,* 2017; Muccillo, Netto, and Muccillo, 2001). Calcia can be produced from lime which is extremely abundant in the world. In 2018, the world production of lime reached 420 million tons, but the production of yttria is only 5,000 to 7,000 tons which are entirely centralized in China (USGS, 2019). In industrial applications, calcia-stabilized zirconia (CSZ) is regularly used to measure oxygen partial pressure in situ in metal, glass, and refractory processing at high temperatures (Zhou and Ahmad, 2006).

Generally, there are three types of SOFC cell design consisting of electrolyte-supported, electrode-supported, and metal-supported. The electrolyte-supported design offers high mechanical strength and avoid side reaction between conventional cathodes such as LSM or LSCF and zirconia-based electrolyte during the sintering process (Stolten and Emonts, 2012). However, the design requires a high operating temperature to decrease ohmic resistance. Moreover, in electrode configuration, anode-supported design is more popular than cathode-supported design owing to ease of fabrication, high electrical conductivity, low operating temperature, and cost-effective design. Moreover, the disadvantage of the anode-supported design is the large volume change due to the reduction process during operation, making it prone to electrolyte cracking (Roehrens *et al.,* 2015; Islam and Hill, 2013).

Another phenomenon that causes a crack in the electrolyte is curvature during half-cell sintering in an anode-supported design. The curvature occurs due to the difference in thermal expansion and sintering rates of the anode and electrolyte (Cologna *et al.,* 2010). To sort out curvature, the thickness of the electrolyte should be controlled. In the anode-supported configuration, the thin-film electrolytes are produced through some techniques such as chemical vapor deposition (CVD) (Gelfond *et al.,* 2009), DC sputtering (Sonderby *et al.,* 2015), and spray coating (Abarzua *et al.,* 2021). Among the methods, spray coating is a low-cost technique for the mass production of thin electrolytes in anode-supported cells. Previous studies showed that this method could produce thin dense electrolytes with less than 50 μm of thickness, and the electrolyte film was stable during testing (Yang, Zhang, and Yan, 2022).

Our previous SOFC had greatly poor electrochemical (ohmic resistance up to 3,624 Ω and 0.001 mW/cm^2 of maximum power density) and mechanical performance (0 Mohs of hardness) since the electrolyte and anode structure are too porous (Widiatmoko *et al.,* 2019). In this work, we exhibited an enhancement to our previous work by the fabrication

and characterization of an anode-supported SOFC single cell using NiO-CSZ anode, CSZ electrolyte, and CCZO-CSZ cathode with the different pore-former composition, powder mixing method, sintering condition, and amount of electrolyte coating from our previous work. These parameters were the key to producing the robust anode as a support and the dense and thin electrolyte.

2. Materials and Methods

2.1. Powder Preparation

Firstly, electrolyte powder was prepared by mixing 3 wt.% of CaO from Bratachem (technical grade, Bandung, Indonesia) and 97 wt.% of ZrO_2 purchased from Pingxiang Ball-Tec New Materials Co., Ltd (technical grade, Jianxi, China) with 1 wt.% of polyethylene glycol (PEG) as a plasticizer, polyvinyl alcohol (PVA) as a binder and ethanol from Bratachem (technical grade, Bandung, Indonesia) as a medium in a ball mill and mixer. Secondly, the anode powder consisting of 65 wt.% of NiO purchased from Changsha Easchem Co., Ltd (technical grade, Changsa, China), 35 wt.% of CSZ, 1 wt.% of PVA and corn starch (0, 10, and 15 wt.%) was mixed at ball mill and mixer with ethanol. Lastly, to produce CCZO cathode powder, CaO, Co_3O_4, and ZnO from Bratachem (technical grade, Bandung, Indonesia), weighed in a stoichiometric amount, were blended with 1 wt.% of PVA, PEG, and ethanol in a ball mill. The drying of all powders is carried out at 100 °C for 24 h.

2.2. Cell Fabrication

To produce an anode-supported IT-SOFC, the anode powder was molded through dry pressing with a load of 8 tons for 5 minutes. The dimension of the anode was 40 mm in diameter. The NiO-CSZ anode was sintered at 1,100 °C for 3 h. Electrolyte and cathode powders were mixed with isopropyl alcohol (IPA) as a dispersant to form a slurry. The electrolyte slurry was coated onto the anode surface using the spray coating method at a pressure of 2 bar and continued heating in the oven for 1 h to remove dispersants. The lining process of the electrolyte was done once and eight times by coating. The CSZ electrolyte was sintered at 1,100 °C for 3 and 2 h. Moreover, the cathode slurry was coated onto the anode-electrolyte surface using a spray coating technique with an effective area of 7 cm^2. The sintering of the CCZO cathode was carried out at 900 °C for 5 h.

2.3. Physical Characterization

The porosity of the anode was determined by ASTM C373-88, while the microstructure of the cells was observed by scanning electron microscope (SEM, Hitachi SU3500, Hitachi High-Technologies Corporation, Japan). The hardness of NiO-CSZ anodes was tested by the Mohs method using SNI 7275-2008 in the Center for Ceramics, Indonesia. In addition, the curvature was examined with angle measurement and the value of curvature was calculated by using Equation (1) (Nguyen *et al.,* 2016):

$$\text{Curvature (flatness)} = b - a \quad (1)$$

Where b is the height from the flat surface to the top of the curved substrate, and a is the thickness of the half-cell sample.

2.4. Electrochemical Characterization

The electrochemical test was performed in stainless steel (SS) 316L frame and sealed with ceramic paper and castable refractory cement C-18. SS 304 mesh was used as a current collector in the anode and cathode sides. The anode was reduced from NiO to Ni at 800 °C with pure hydrogen. Anode-supported cells were characterized at 600, 700, and 800 °C using hydrogen as a fuel and ambient air as an oxidant with a flow rate of 200 and 2,000 ml/min, respectively. The impedance cell was measured at a frequency range from 100 kHz

to 0.1 Hz under an open-circuit voltage (OCV) condition. Current-voltage characteristics and impedance at each temperature were carried out by Gamry V3000 potentiostat (Gamry Instruments, USA). Figure 1 exhibits a schematic of the setup for cell testing.

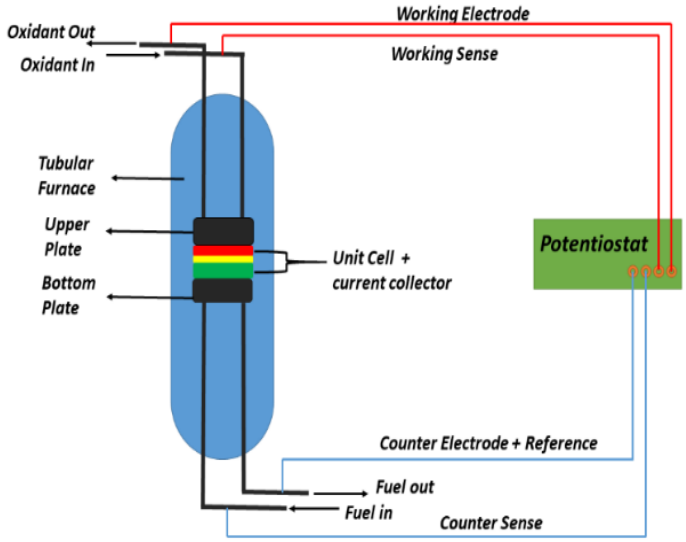

Figure 1 A schematic of SOFC single-cell testing using a tubular furnace connected to a potentiostat

3. Results and Discussion

3.1. Porosity and Microstructure

Table 1 illustrates the effect of the amount of pore former on the porosity and hardness of anode sintered at 1,100 °C for 3 h. The porosity of the anode before reduction without a pore-forming agent was 9.8%, while with the pore-forming agent was 24.7% for 10 wt.% of corn starch, 1 wt.% of PVA and 40.1% for 15 wt.% of corn starch, 1 wt.% of PVA. Moreover, the hardness of the cermet without pore former was 7 Mohs, while with pore former was 1 Mohs for 10 wt.% of corn starch, 1 wt.% of PVA, and 0 Mohs for 15 wt.% of corn starch, 1 wt.% of PVA. The porosity of sintered anode increases with the increasing amount of corn starch.

Table 1 Effect of amount of pore former on the porosity and hardness of anode sintered at 1,100 °C for 3 h

Corn starch (wt%)	PVA (wt%)	Porosity before reduction (%)	Hardness (Mohs)
0	0	9.8	7
10	1	24.7	1
15		40.1	0

Additionally, PVA can act as not only a binder but also a pore former (Amiri and Paydar, 2017). According to the literature, an increase in the porosity of anode after reduction with corn starch and PVA as pore former can reach up to 18% (Batool *et al.,* 2018; Ding *et al.,* 2016). The recommended SOFC anode should have a 30-40% porosity after reduction to obtain high electronic conductivity, desired electrochemical characteristics, and higher gas diffusion to triple phase boundary (TPB) (Horri, Selomulya, and Wang, 2012). However, the high weight percentage of the pore former decreases the hardness of the anode. It showed the strength of the anode as a support to prevent cracking during cell testing and operation. From our previous work (Widiatmoko *et al.,* 2019), the anode sintered at 1,000 °C for 5 h with 15 wt.% of corn starch and 1 wt.% of PVA was chosen as support resulting in poor

mechanical strength of the anode due to the high amount of pore-forming agent and low-temperature sintering. Therefore, in this study, the NiO-CSZ cermet sintered at 1,100 °C for 3 h with 10 wt.% of corn starch and 1 wt.% of PVA was selected as a supported substrate.

Figure 2 shows a cross-sectional and surface view of the anode-supported single cell before testing. The thickness of the anode and cathode was ~1.1 mm and ~34.8 µm, respectively. Figure 2a and 2b clearly shows that the morphology of NiO-CSZ cermet and CCZO-CSZ composite was porous. In addition, the particle size of the anode was much bigger than that of the cathode since the sintering temperature of the cathode was lower than that of the anode (900 °C versus 1,100 °C) (Joo and Choi, 2008). The particle size of the NiO-CSZ anode and CCZO-CSZ cathode was ~1.2 and ~0.5 µm, respectively. Meanwhile, in the electrolyte part, the microstructure with eight times of coating was denser than that with one time of coating, as shown in Figures 2d and 2e. The thickness of electrolyte with one time and eight times of coating was ~17.0 and ~87.2 µm, respectively. The CSZ electrolyte film will be thicker with the increasing amount of coating process repetition. However, the sintered electrolyte with eight times coating still had a porous structure, and the film thickness of the electrolyte and cathode was not uniform.

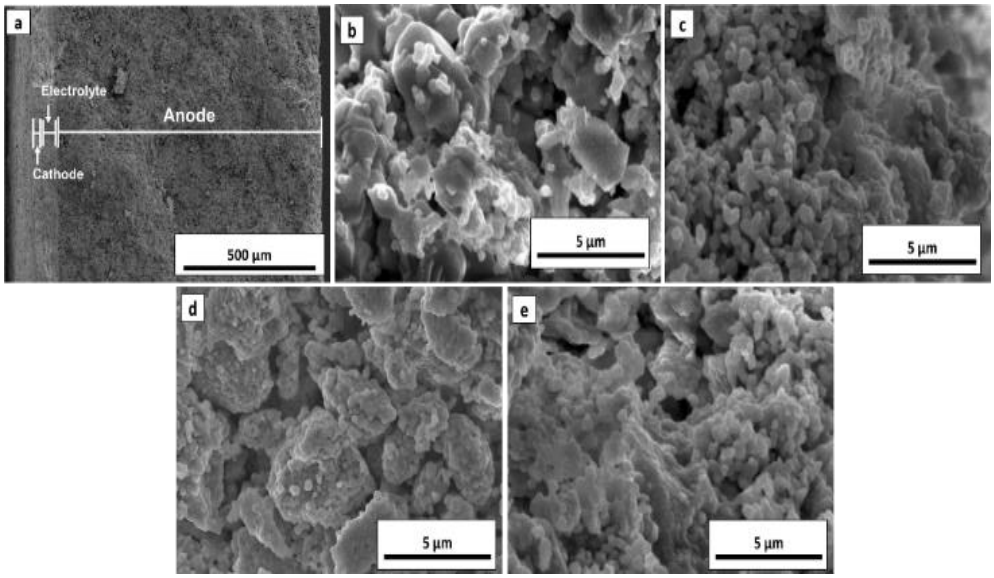

Figure 2 SEM micrograph of the (a) cross-section of an electrolyte-supported IT-SOFC cell before testing; (b) surface view of NiO-CSZ anode; (c) CCZO cathode; CSZ electrolyte with (d) one time; and (e) eight times of coating

3.2. Curvature of Anode-Electrolyte Cell

In anode and electrolyte powder preparation, a mixer and ball mill were used as mixing equipment. The sintering process of half-cell (anode-electrolyte), particularly in the anode-supported cell, is the potential for curvature phenomenon. Figure 3 and Table 2 revealed curvature photograph and value in half-cell using a mixer and ball mill in powder preparation with a different dwell time of sintering and amount of electrolyte coating. The half-cell with a mixer in powder preparation shown in Figure 3a has a different angle on both sides. The powder blending with the mixer was not homogenous, so the thermal expansion did not spread uniformly. Meanwhile, the anode-electrolyte cell with ball mill in powder preparation shown in Figure 3b has a similar angle on both sides even though the angle of this half-cell was larger than that of the half-cell with mixer. The curvature value of anode-electrolyte cell sintered at 1,100 °C for 3 h with a mixer and ball mill in powder preparation was 0.89 and 1.18 mm, respectively, as shown in Table 2. This confirmed that the bigger the angle is, the higher the curvature value is. This phenomenon means the

anode-electrolyte cell with a ball mill in powder preparation produces homogenous mixtures (Malzbender, Wakui, and Steinbrech, 2006). Additionally, it is reasoned that the sintering rate of the electrolyte was larger than the anode, which could not resist forces applied to the anode by electrolyte sintering (Lankin and Karan, 2009).

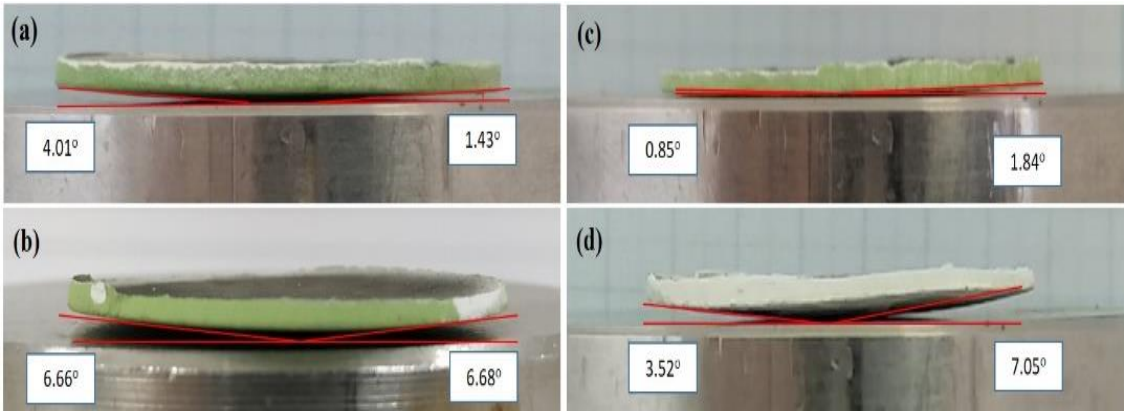

Figure 3 Curvature of anode-electrolyte cell sintered at 1,100 °C for 3 h using (a) mixer; (b) ball mill in preparation; for 2 h using ball mill in preparation with (c) one time; and (d) eight times of electrolyte coating

The study by (Cologna *et al.*, 2009) reported the curvature could be solved by reducing the dwell time of half-cell sintering. In Figure 3c, the dwell time of anode-electrolyte sintering decreased from 3 to 2 h. The picture exhibited the angle on both sides was lesser than the angle in half-cell with a dwell time of 3 h. The curvature value reduced by ~62% when the dwell time of sintering decreased. It is clear that the shorter the anode-electrolyte sample is held at the sintering temperature, the lesser the curvature occurs. However, when the dwell time of electrolyte sintering decreases, the electrolyte densification will be worse. On the other hand, Figure 3d showed that the half-cell with eight times of electrolyte coating curved sharply on both sides compared with the half-cell with one time of electrolyte coating, as shown in Figure 3c. The curvature value of half-cell with eight times of electrolyte coating increased by about 66%. Hence, the thick electrolyte layer enforces greater stress on the anode, causing an increase in curvature (Ruhma *et al.*, 2021).

Table 2 Curvature value of four half-cell substrates sintered at 1,100 °C with different mixing methods, dwell time of sintering, and amount of coating electrolyte

Mixing Method	Amount of Electrolyte Coating	Dwell Time of Sintering (h)	b (mm)	a (mm)	Curvature (mm)
Mixer	Once	3	2.04	1.15	0.89
Ball Mill		3	2.33	1.15	1.18
		2	1.60	1.15	0.45
	Eight times	2	2.54	1.20	1.34

3.3. Electrochemical Performance

Polarization curves of anode-supported cells with one time and eight times of electrolyte coating at 800 °C were shown in Figure 4. The OCV of a single cell with eight times of electrolyte coating was greater than that with one time of electrolyte coating. However, the OCV of the cells was significantly lower than the theoretical OCV based on the Nernst equation. The dropped voltage is led to fuel and oxidant crossover phenomenon and gas leakage through sealant to the environment (Rasmussen, Hendriksen, and Hagen, 2008; Suzuki *et al.*, 2005). Moreover, the current densities of cells with one time and eight times of electrolyte coating achieved about 14 and 10 mA/cm^2, respectively. When the electrolyte

was thick, the resistance was so high that the current density of the cell declined. The peak power densities of anode-supported cells with one time and eight times of electrolyte coating were 0.94 and 1.08 mW/cm^2, respectively. Moreover, Figure 5 presented the performance of an anode-supported cell with eight times of electrolyte coating at different operating temperatures (600, 700, and 800 °C). The values of maximum power density at 600, 700, and 800 °C were 0.24; 0.35; and 1.08 mW/cm^2, respectively. Peak power density decreases, and OCV increases with a lowering operating temperature. Additionally, the peak power density at 700 °C boosted about 350 times higher than that of our previous work from 0.001 to 0.35 mW/cm^2 (Widiatmoko *et al.,* 2019).

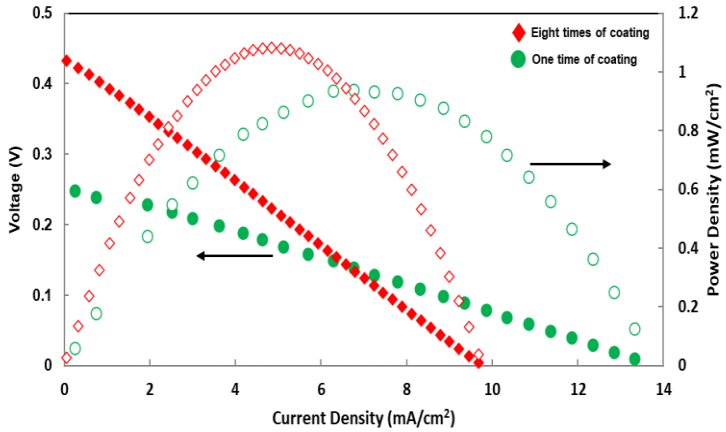

Figure 4 Polarization curves of anode-supported cell with one time and eight times of electrolyte coating at 800 °C

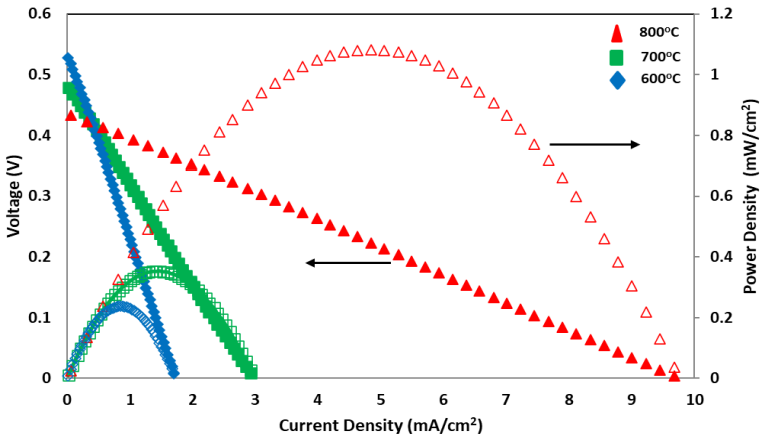

Figure 5 Polarization curves of anode-supported cell with eight times of electrolyte coating at different temperatures.

Impedance measurements of the cell were performed under OCV, and the curves were fitted with an equivalent circuit model, as shown in Figure 6. Ohmic resistances (Rohm) of the cell at 600, 700, and 800 °C were 168.30; 90.10; and 26.78 Ω, respectively, as summarized in Table 3. The thick electrolyte layer leads to high ohmic resistance of the single cell (Park *et al.,* 2018).

On the other hand, the polarization resistance (Rp) values, including charge and mass transfer, of 155.10; 103.56; and 11.57 Ω were gained at 600, 700, and 800 °C, respectively. Conductivity and gas diffusion in the anode and cathode were responsible for high polarization resistance (Troskialina, 2015). Moreover, Rohm and Rp values were significantly lower in this work than in our previous work. Hence, the improvement in the fabrication of anode-supported IT-SOFC cells enhanced electrochemical performance.

Overall, compared with our previous study, the maximum power density of the cell at 700 °C was ~350 times higher, while ohmic and polarization resistance at 700 °C was highly reduced at ~40 times and ~500 times, respectively.

Table 3 Summary of resistance values extracted from an equivalent circuit model at 600, 700, and 800 °C under OCV condition

T (°C)	R_{ohm} (Ω)	$R_p = R_1+R_2$ (Ω)	R_1 (Ω)	R_2 (Ω)
600	168.30	155.10	98.22	56.88
700	90.10	103.56	97.70	5.86
700 (our previous work)	3,624	54,670	22,750	31,920
800	26.78	11.57	5.86	5.71

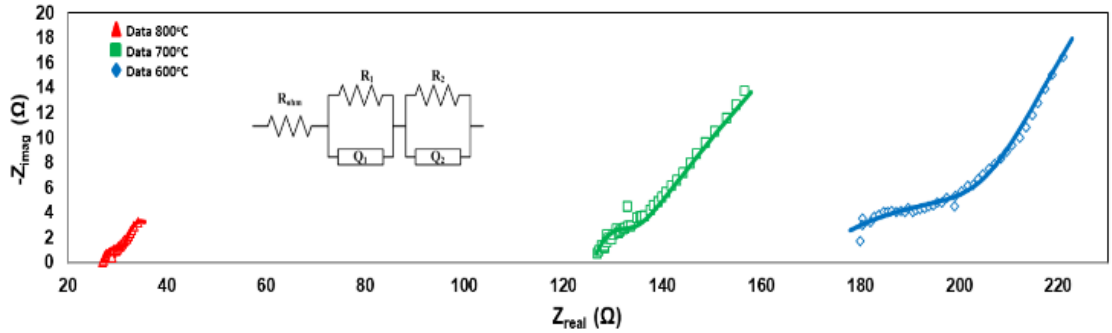

Figure 6 Electrochemical impedance spectra and equivalent circuit model of the anode-supported single cell at 600, 700, and 800 °C under OCV condition

4. Conclusions

The anode-supported single cell consisting of NiO-CSZ anode, CSZ electrolyte, and CCZO-CCZO cathode was successfully improved both in electrochemical and mechanical characteristics. The porosity of the anode is sufficient to obtain a robust structure and to allow fuel gas diffusion to TPB. Meanwhile, electrolytes with eight times of coating still had a porous structure which is highly potential to fuel and oxidant crossover phenomenon. On the other hand, curvature was overcome by reducing the dwell time of sintering, but when the electrolyte film was thick, the curvature increased two times/twice. In electrochemical performance, peak power density, Rohm, and Rp at 800 °C was 1.08 mW/cm^2, 26.78 Ω, and 11.57 Ω, respectively. However, the spray-coated CSZ single cell was still lower than commercial YSZ-based SOFC cell. In future studies, the CSZ electrolyte fabrication technique is key to making denser and thin electrolytes to avoid fuel crossover.

Acknowledgments

The authors would like to thank the financial support provided by Institut Teknologi Bandung through Research, Community Service, and Innovation ITB 2019 Program (Contract No: 0922b/I1.C06.2/PL/2019) and the support of laboratory facilities provide by Center for Hydrogen-Fuel Cell Research, Korea Institute of Science and Technology (KIST).

References

Abarzua, G., Udayabhaskar, R., Mangalaraja, R.V., Durango-Petro, J., Usuba, J., Flies, H., 2021. A Feasible Strategy for Tailoring Stable Spray-Coated Electrolyte Layer in Micro-

Tubular Solid Oxide Fuel Cells. *International Journal of Applied Ceramic Technology*, Volume 19(3), pp. 1389–1396. doi: 10.1111/ijac.13981

Abdalla, A.M., Hossain, S., Azad A.T., Petra, P.M.I., Begum, F., Eriksson, S.G., Azad, A.K., 2018. Nanomaterials for Solid Oxide Fuel Cells: A Review. *Renewable & Sustainable Energy Reviews*, Volume 82, pp. 353–368. doi: 10.1016/j.rser.2017.09.046

Amiri, S., Paydar, M.H., 2017. Effect of Pore Formers Characteristics and Melt Infiltration Parameters on Microstructure and Electrical Properties of $BaCe_{0.7}Zr_{0.1}Y_{0.2}O_{3-\delta}$-Carbonate Composite Electrolyte. *Journal of Alloys and Compounds*, Volume 735, pp. 172–183. doi: 10.1016/j.jallcom.2017.11.067

Baharuddin, N.A., Muchtara, A., Somalu, M.R., 2017. Short Review on Cobalt-Free Cathodes for Solid Oxide Fuel Cells. *International Journal of Hydrogen Energy*, Volume 42, pp. 9149–9155. doi: 10.1016/j.ijhydene.2016.04.097

Batool, M., Sattar, M., Barki, U.K., Khan, Z.S., 2018. Synthesis of Ni/YSZ Based Anode and Investigation of Effect of PVA as Pore-Former Upon Porosity, Microstructure and Thermal Behavior for Potential Use In Solid Oxide Fuel Cells (SOFCs). *International Journal of Materials Research*, Volume 109, pp. 1153–1159. doi: 10.3139/146.111713

Chen, Y., Yang, L., Ren, F., An, K., 2014. Visualizing the Structural Evolution of LSM/xYSZ Composite Cathodes for SOFC by in-Situ Neutron Diffraction. *Scientific Reports,* Volume 4(1), p. 5179. doi: 10.1038/srep05179

Cologna, M., Contino, A.R., Montinaro, D., Sglavo, V.M., 2009. Effect of Al and Ce doping on the deformation upon sintering in sequential tape cast layers for solid oxide fuel cells. *Journal of Power Sources*, 193, pp. 80-85. doi: 10.1016/j.jpowsour.2008.12.052

Cologna, M., Contino, A.R., Sglavo, V.M., Modena, S., Ceschini, S., Bertoldi, M., 2010. *Curvature Evolution and Control in Anode Supported Solid Oxide Fuel Cells in Advances: Solid Oxide Fuel Cells V*. New Jersey: John Wiley & Sons, Inc. doi: 10.1002/9780470584316.ch8

Ding, C., Zhang, J., Liu, Y., Gou, J., Luan, J., 2016. Effects of Pore-Forming Agent on Characterization of NiO/YSZ Porous Anode for SOFC. *Materials Science Forum*, Volume 848, pp. 389–395. doi: 10.4028/www.scientific.net/MSF.848.389

Gelfond, N.V., Bobrenok, O.F., Predtechensky, M.R., Morozova, N.B., Zherikova, K.V., Igumenov, I.K., 2009. Chemical Vapor Deposition of Electrolyte thin Films Based on Ytrria-Stabilized Zirconia. *Inorganic Materials*, Volume 45(6), pp. 659–665. doi: 10.1134/S0020168509060144

Horri, B.A., Selomulya, C., Wang, H., 2012. Characteristics of Ni/YSZ Ceramic Anode Prepared using Carbon Microspheres as a Pore Former. *International Journal of Hydrogen Energy*, Volume 37, pp. 15311–15319. doi: 10.1134/S0020168509060144

Islam, S., Hill, J.M., 2013. Anode Materials Development. In*: Solid Oxide Fuel Cells: From Materials to System Modeling.* London: RSC Publishing. doi: /10.1039/9781849737777

Joo, J.H., Choi, G.M., 2008. Thick-Film Electrolyte (thickness <20 μm)-Supported Solid Oxide Fuel Cells. *Journal of Power Sources*, Volume 180, pp. 195–198. doi: 10.1016/j.jpowsour.2008.02.013

Kaur, P., Singh, K., 2020. Review of Perovskite-Structure Related Cathode Materials for Solid Oxide Fuel Cells. *Ceramic International*, Volume 46, pp. 5521–553. doi: 10.1016/j.ceramint.2019.11.066

Lankin, M.K., Karan, K., 2009. Effect of Processing Conditions on Curvature of Anode/Electrolyte SOFC Half-Cells Fabricated by Electrophoretic Deposition. *Journal of Electrochemical Energy Conversion and Storage*, Volume 6, p. 021001. doi: 10.1115/1.2971044

Kurapova, O.Y., Glumov, O.V., Pivovarov, M.M., Golubev, S.N., 2017. Structure and Conductivity of Calcia Stabilized Zirconia Ceramics, Manufactured from Freeze-Dried

Nanopowder. *Reviews on Advanced Material Science*, Volume 52, pp. 134–141. doi: 222174886

Malzbender, J., Wakui, T., Steinbrech, W., 2006. Curvature of Planar Solid Oxide Fuel Cells During Sealing and Cooling of Stacks. *Fuel Cells*, Volume 6, pp. 123–129. doi: 10.1002/fuce.200500109

Muccillo, R., Netto, R.C., Muccillo, E.N., 2001. Synthesis and Characterization of Calcia Fully Stabilized Zirconia Solid Electrolytes. *Material Letters*, Volume 49, pp. 197–201. doi: 10.1016/S0167-577X(00)00367-0

Nguyen, X-V., Chang, C-T., Jung, G-B., Chan, S-H., Huang, W. C-W., Hsiao, K-J., Lee, W-T., Chang, S-W., Kao, I-C., 2016. Effect of Sintering Temperature and Applied Load On Anode-Supported Electrodes for SOFC Application. *Energies*, Volume 9, pp. 1–13. doi: 10.3390/en9090701

Park, J.M., Kim, D.Y., Baek, J.D., Yoon, Y.J., Su, P.C., Lee, S.H., 2018. Effect of Electrolyte Thickness on Electrochemical Reactions and Thermo-Fluidic Characteristics Inside A SOFC Unit Cell. *Energies*, Volume 11(473), pp. 1–25. doi: 10.3390/en11030473

Rahmawati, F., Permadani, I., Syarif, D.G., Soepriyanto, S., 2017. Electrical Properties of Various Composition of Yttrium Doped-Zirconia Prepared from Local Zircon Sand. International Journal of Technology. Volume 8(5), pp. 939–946. doi: 10.14716/ijtech.v8i5.876

Rasmussen, J.F.B., Hendriksen, P.V., Hagen, A., 2008. Study of Internal and External Leaks in Tests of Anode-Supported SOFCs. *Fuel Cells*, Volume 8, pp. 385–393. doi: 10.1002/fuce.200800019

Roehrens, D., Han, F., Haydn, M., Schafbauer, W., Sebold, D., Menzler, N.H., Buchkremer, H.M., 2015. Advances Beyond Traditional SOFC Cell Designs. *International Journal of Hydrogen Energy*, Volume 40(35), pp. 11538–11542. doi: 10.1016/j.ijhydene.2015.01.155

Ruhma, Z., Yashiro, K., Oikawa, I., Takamura, H., Kawada, T., 2021. Metal-supported SOFC Fabricated by Tape Casting andIts Characterization: A Study of the Co-sintering Process. *Journal of Engineering and Technological Sciences*, Volume 53(5), pp. 991–1013. doi: 10.5614/j.eng.technol.sci.2021.53.5.11

Sazali, N., Salleh, W.N.W., Jamaludin, A.S., Razali, M.N.M., 2020. New Perspectives on Fuel Cell Technology: A Brief Review, *Membranes*, 10, pp. 1–18. doi: 10.3390/membranes10050099

Shi, H., Su, C., Ran, R., Cao, J., Shao, Z., 2020. Electrolyte Materials for Intermediate-Temperature Solid Oxide Fuel Cells. *Progress in Natural Science: Materials International*, Volume 30(6), pp. 764–774. doi: 10.1016/j.pnsc.2020.09.003

Singhal, S.C., Kendall, K., 2003. *High-temperature Solid Oxide Fuel Cells: Fundamentals, Design and Applications*. Oxford: Elsevier Ltd. doi: 10.1016/B978-1-85617-387-2.X5016-8

Sonderby, S., Christensen, B.H., Almtoft, K.P., Nielsen, L.P., Eklund, P., 2015. Industrial-Scale High Power Impulse Magnetron Sputtering of Yttria-Stabilized Zirconia on Porous NiO/YSZ Fuel Cell Anodes*. Surface and Coatings Technology*, Volume 281, pp. 150–156. doi: 10.1016/j.surfcoat.2015.09.058

Stolten, D., Emonts, B., 2012. *Fuel Cell Science and Engineering: Materials, Processes, Systems and Technology.* New Jersey: Wiley. doi: 10.1002/9783527650248

Suzuki, T., Jasinski, P., Petrovsky, V., Anderson, H.U., 2005. Performance of a Porous Electrolyte in Single-Chamber SOFCs. *Journal of Electrochemical Society*, Volume 152, pp. 27–31. doi: 10.1149/1.1858811

Takami, T., Ikuta, H., 2005. Thermoelectric Properties of One-Dimensional Cobalt Oxide $Ca_3Co_2O_6$ and The Effect of Zn Doping, *In:* 24th International Conference on Thermoelectrics, pp. 480–483. doi: 58509459

Troskialina, L., 2015. *Improved Performance of Solid Oxide Fuel Cell Operating on Biogas using Tin Anode-infiltration.* PhD Dissertation, School of Chemical Engineering., University of Birmingham., Birmingham. Accessed via: https://etheses.bham.ac.uk/id/eprint/6790/1/Troskialina16PhD.pdf

U.S. Geological Survey (USGS), 2019. *Mineral Commodity Summaries 2019*. U.S. Geological Survey, Virginia. doi: 10.3133/70202434

Wang, S., Jiang, S.P., 2017. Prospects of Fuel Cell Technologies. *National Science Review*, Volume 4, pp. 163–166. doi: 10.1093/nsr/nww099

Widiatmoko, P., Devianto, H., Nurdin, I., Yusupandi, F., Kevino., Ovani, E.N., 2019. Fabrication and Characterization of Intermediate-Temperature Solid Oxide Fuel Cell (IT-SOFC) Single Cell Using Indonesia's Resources. *IOP Conference Series: Materials Science and Engineering,* Volume 550, pp. 1–6. doi: 10.1088/1757-899X/550/1/012001

Yang, Y., Zhang, Y., Yan, M., 2022. A Review on the Preparation of Thin-Film YSZ Electrolyte of SOFCs by Magnetron Sputtering Technology. *Separation and Purification Technology*, Volume 298, p. 121627. doi: 10.1016/j.seppur.2022.121627

Yu, S., Zhang, G., Chen, H., Guo, L., 2017. A Novel Post-Treatment to Calcium Cobaltite Cathode for Solid Oxide Fuel Cells. *International Journal of Hydrogen Energy*, Volume 43, pp. 2436–2442. doi: 10.1016/j.ijhydene.2017.12.040

Zhou, M., Ahmad, A., 2006. Synthesis, Processing and Characterization of Calcia-Stabilized Zirconia Solid Electrolytes for Oxygen Sensing Applications. *Material Research Bulletin*, Volume 41, pp. 690–696. doi: 10.1016/j.materresbull.2005.10.018